ELSEVIER

Chemical Engineering Journal 136 (2008) 390–397

Chemical Engineering Journal

www.elsevier.com/locate/cej

Preparation of Au-CeO_2 and Au-Al_2O_3/AISI 304 austenitic stainless steel monoliths and their performance in the catalytic oxidation of CO

L.M. Martínez T[a,*], D.M. Frías[b], M.A. Centeno[a], A. Paúl[a], M. Montes[b], J.A. Odriozola[a]

[a] *Departamento de Química Inorgánica e Instituto de Ciencia de Materiales de Sevilla, Universidad de Sevilla-CSIC, Avda. Américo Vespucio 49, 41092 Sevilla, Spain*

[b] *Grupo de Ingeniería Química, Dpto. Química Aplicada, Fac. Ciencias Químicas de San Sebastián, UPV/EHU, Paseo Manuel de Lardizábal 3, 20018 San Sebastián, Spain*

Received 7 February 2007; received in revised form 18 May 2007; accepted 21 May 2007

Abstract

The use of austenitic stainless steel (AISI 304) as metallic substrate for monolithic catalytic devices is explored in this work as well as an alternative procedure to the washcoating of Al_2O_3 and CeO_2 supported Au catalysts. Thermal treatment of the metallic surface ensured a good adherence of the catalysts. Some preparation parameters, like the number of dipping and drying steps, were controlled in order to obtain an homogeneous and adherent layer of catalyst. The resulting surfaces were characterized by X-ray diffraction (XRD), N_2 sorption and scanning electron microscopy (SEM), and were tested in the CO oxidation reaction. The highest conversion to CO_2 was obtained with the monolith coated with 1% Au-CeO_2 in the presence of water.
© 2007 Elsevier B.V. All rights reserved.

Keywords: Metallic monolith; Austenitic stainless steel; Gold catalysts; CO oxidation

1. Introduction

Nowadays, the use of the monolithic catalysts has become frequent [1]. Among the reported uses, their application in environmental catalysis increase continuously. Monolithic catalysts have the advantages of a low energy input (one-tenth of that of the packed-bed reactor because of the straight channels), a high catalytic performance per mass unit of active phase, safer operating conditions and easiest catalyst separation [2–4]. Monolithic catalysts can be prepared directly by extruding plastic pastes of the active phase, but, in general, they are prepared by deposition of the active layer on a preformed monolithic support. Carbon, ceramic materials (cordierite or silica) or metallic ones (i.e. aluminium, ferritic alloys) have been described as appropriate supports [2]. Typically, the monolithic support is coated with a material of high surface area which acts as a host for the active metal catalysts [5]. An adequate adhesion of the washcoated layer to the substrate is a crucial requirement, since the conditions of operation (hot exhaust gases at high velocity and mechanical vibrations), may lead to active layer spalling, with the consequent degradation of the catalyst efficiency. Concerning the nature of the support, ceramics monoliths have been widely used due to the easiness of the deposition of the active phase, although they show some limitations compared to the use of metallic ones, such as a higher wall thickness (≈100 μm), a higher fragility and a much lower thermal and electrical conductivities [2]. An additional advantage of the use of a metallic substrate is machinability, which allows the fabrication of devices with designs adapted to final use. However, metallic monoliths present a low adherence of the washcoating. In order to improve this adherence, a suitable treatment for the metallic substrate is required. Ferritic alloys containing 3–5% of aluminium (for instance, Fecralloy®) produce an Al_2O_3 layer by thermal [2,5] or chemical [6] treatment that favors the interaction of the catalytic coating. A porous alumina layer is also produced by anodization of pure aluminium [7]. Austenitic stainless steels become in an interesting alternative to the use of Fecralloy® and aluminium substrates for fabrication of metallic monoliths for low temperature applications. Austenitic stainless steels are cheap and can be used at temperatures as high as 1023 K, thus they might be used at the normal operation temperatures expected in environmental catalytic processes. In addition,

* Corresponding author.
E-mail address: leidy@icmse.csic.es (L.M. Martínez T).

1385-8947/$ – see front matter © 2007 Elsevier B.V. All rights reserved.
doi:10.1016/j.cej.2007.05.040

the thermal treatment needed to improve the adherence of the washcoated active phase to the austenitic stainless steel, generates a scale of metal transition oxides such as Cr, Fe or Mn [8,9], which could present catalytic activity in oxidation reactions [10].

The main objective of this work is to describe the guidelines for the rational selection of the preparation method in order to obtain an homogeneous and adherent catalytic layer on AISI 304 stainless steels. Au-CeO_2 and Au-Al_2O_3 were selected as active phases and the prepared monoliths were tested in the catalytic oxidation of CO as a test reaction.

2. Experimental

2.1. Sample preparation

A commercial AISI 304 austenitic stainless steel sheet (50 μm thick) was used as raw material. Table 1 shows a typical compositional analysis. Monoliths were prepared by rolling around a spindle alternate flat and corrugated sheet [2]. The final monolith is a cylinder of 30 mm height, 16 mm diameter and a cell density of 55 cell/cm^2.

Before coating, metallic monoliths were pretreated to generated and adequate surface for washcoating by thermal heating in 10 ml/min flow of synthetic air (Air Liquide, 99.999 pure) from room temperature to 1173 K at 10 K/min, maintained 60 min at this temperature and then cooled down to room temperature under the same atmosphere.

Commercial colloidal solutions of cerium acetate and bohemite (Nyacol) were used. In order to optimize the rheological properties of the colloidal solutions to improve the homogeneity of the catalytic deposit and to avoid cracking effects of the layer, the initial concentration of solids in the colloidal solutions was adjusted to 10 wt% CeO_2, in the case of cerium solution, and 15 wt% Al_2O_3 in the case of the bohemite one [11]. For deposition of the Au catalysts, the adequate amount of gold acetate (Alfa Aesar 99.99%) to obtain a gold concentration of 0.1 and 1 wt% in the final solid, was added to the colloidal solutions and mixed before the monolith coating procedure begins. The use of gold acetate as source of gold instead of the normally used for powder gold catalysts preparation (chloroauric acid) is needed, since chloride ions attack the stainless steel surface producing pitting corrosion. The coating procedure consists in the immersion of the monolith in the adequate colloidal solutions for 1 min and then withdrawn at a constant speed of 3 cm/h. To avoid obstruction of the monoliths channels, the excess of colloid was removed by centrifugation at 400 rpm for 10 min. The obtained coated monoliths were dried by freeze-drying during 4 h, and finally calcined 4 h at 773 K at a heating rate of 2 K/min. This drying and calcination procedure has been shown as the best one to obtain an homogenous and well adhered catalytic layer on the oxidized metallic substrate [11]. To increase the amount of catalysts loaded on the monoliths (∼100 mg), up to three successive coating, drying and calcinations procedures were carried out.

Powder catalysts were obtained by drying at 353 K and further calcination at 773 K, of the corresponding colloidal solutions.

Table 1
Composition of the commercial AISI 304 stainless steel sheet used (Fe balance)

Element	wt%
Cr	18.4
Ni	8.11
Si	0.44
Mn	1.45
N	0.057
C	0.064
Cu	0.23
Mo	0.25
P	0.03
S	0.001
Co	0.2
V	0.13
W	0.15

2.2. Characterization

The textural properties were studied by N_2 adsorption measurements at liquid nitrogen temperature in a Micromeritics ASAP 2010 apparatus between 0.1 and 0.995 mmHg with a homemade cell that allows analyzing the complete monolith. Before analysis, the monoliths were degassed for 2 h at 423 K in vacuum.

X-ray diffraction (XRD) were recorded using a X'Pert Pro Philips diffractometer working with Cu Kα radiation ($\lambda = 1.5404$ Å) in continuous scan mode from 20° to 80° of 2θ using 0.05° sampling interval and 1.0 s.

Scanning electron microscopy (SEM) observations were carried out in JEOL 5400 equipment. Before the analysis of cross-sections of the monoliths, the samples were coated with Pt in a Sputter Coater TELSTAR EMITECH K-550 and then electrolitically coated with Ni in order to protect and avoid descaling during grounding and polishing.

The adhesion to the metallic substrate of the oxide layer generated in the pretreatment and the catalytic layers deposited has been evaluated using ultrasonic procedures [2].

Roughness measurements were carried out in a Mitutoyo SJ-201P surface tester.

2.3. Activity measurements

The catalytic oxidation of CO was performed in a conventional continuous flow U-shape glass reactor at atmospheric pressure. The monoliths were placed over glass wool and carborundum (Prolabo). The composition of the inlet and outlet gases was analyzed with a Balzers Omnistar Bentchtop mass spectrometer with capabilities for quantitative analysis. Heated stainless steels tubing was used from reactor to gas analyzer to prevent metal wall mediated reactions and product condensation. The light-off curves of CO oxidation (773 K, 5 K/min) were obtained with a mixture 3.4% CO and 21% O_2 balanced by He at a total flow rate of 42 ml/min. Empty reactor (without monolith) showed no activity under these conditions. The catalytic devices were pre-activated "in situ" at 773 K during 60 min with 21% O_2

in He at a flow of 30 ml/min and then stabilized at room temperature before the light-off curved started. In order to evaluate the influence of water in the catalytic performances of the samples, a second test was carried out in which the reactive stream was saturated with water at room temperature.

Temperature control in exothermic reaction during light off curves is a difficult task. It is usually accepted that combustion proceed adiabatically, and then a significant temperature increase will be produced along the catalyst bed or monolith. In our case, the entry flow will produce a temperature increase of around 170 K at total conversion. Therefore, the best option is to monitor the temperature at the bed or monolith entry and accept a temperature profile proportional to the conversion.

Catalytic measurements over the powder catalysts were carried out in the same operating conditions and equivalent contact time to the monolithic catalysts. For that purpose, a similar amount of catalyst to that of the catalytic layer deposited on the monolith substrate (100 mg) was diluted in a volume of glass balls equal to that occupied by the monolithic devices.

3. Results and discussion

3.1. Thermal pretreatment

Austenitic stainless steels develop a rough metal oxide layer during oxidation which could have the adequate properties for its use as substrate to adhere catalysts [2,7]. AISI 304 austenitic stainless steel monoliths were pretreated by thermal heating at 1173 K under synthetic air flow during 60 min. Fig. 1 presents a typical SEM micrograph of the pretreated surface of the monolith, showing the morphology and homogeneity of the generated oxide layer which is form by irregular shaped crystals with diameter ranging from 0.5 to 1 μm. EDX analysis revealed that they correspond to Cr rich oxides and Cr–Mn spinel-type compounds [12].

The XRD diagram of the non-treated monolith (Fig. 2, trace a) only presents diffraction peaks at $2\theta = 43.7°$, 51.2° and 74.5° characteristics of the austenitic phase with fcc structure. After thermal treatment, the intensity of these peaks decreases as a consequence of the low penetration of the X-rays beam through the oxide layer. Besides this, diffraction peaks due to martensite phase (structure bcc) at $2\theta = 44.8°$, 54.8° and 65.2° appear. The formation of this martensite phase can be explained in terms of changes in the surface composition of the steel. In fact, new diffraction lines ascribed to different chromium and manganese oxides appears (Fig. 2, trace b), among them skolaite (Cr_2O_3, $2\theta = 24.5°$, 33.6°, 54.6°) and $Mn_{1+x}Cr_{2-x}O_{4-x}$ spinel-type compounds ($2\theta = 30°$, 34.96°, 63°). The oxidation of austenitic stainless steel results in the formation of a scale whose main components are octahedral $Mn_{1+x}Cr_{2-x}O_{4-x}$ spinel-type compounds and metal oxides, M_2O_3, being M = Cr, Fe or their mixtures, mainly Cr_2O_3 [12–14]. $Mn_{1+x}Cr_{2-x}O_{4-x}$ is generated in the outermost part of the scale and the Cr_2O_3 platelets remain in the innermost one [13].

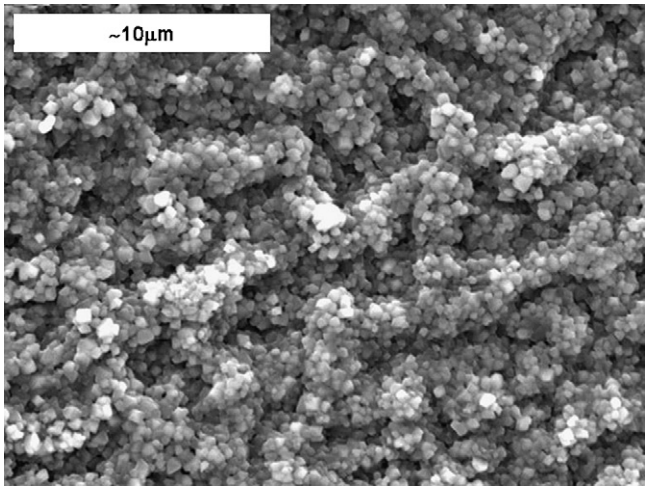

Fig. 1. SEM micrograph of top view of treated AISI 304 austenitic stainless steel monolith at 1173 K for 60 min.

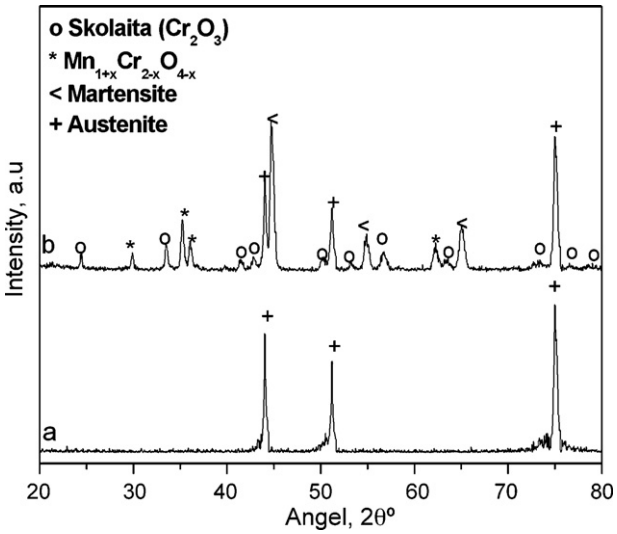

Fig. 2. XRD patterns of AISI 304 austenitic stainless steel monolith: untreated (a) and treated at 1173 K for 60 min (b).

According to the formation of the oxide scale after heating, the roughness of the metallic surface increase from 0.5 to 1.3–1.4 μm. The thickness of this oxide scale is estimated from cross-sectional SEM analyses to be of about 0.75 μm (Fig. 3). Adherence tests put in evidence the good adherence between the scale and the base alloy, since only a 0.08 wt% loss of the scale is observed.

3.2. Catalytic coating

Several methods are available to apply active phase precursors to pre-shaped support, such as impregnation methods, ion exchange and (deposition)–precipitation. Focusing on impregnation methods, three methods are distinguished, pore volume, dry impregnation (incipient wetness) and wet impregnation. In this study, wet impregnation was selected in order to incorporate gold-ceria and gold-alumina catalysts to metallic monoliths. We have selected an one-step washcoating procedure, where gold acetate is added to the colloidal solution of the support (ceria or alumina) before the introduction of the monolith, due to its easiness, the better control of the total amount of gold incorpo-

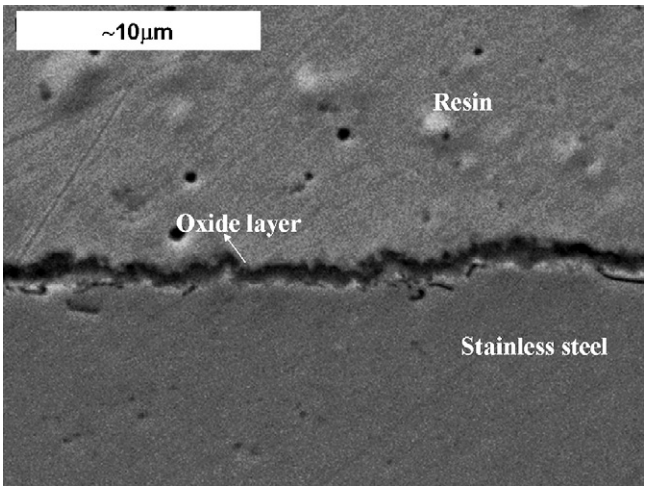

Fig. 3. SEM micrograph of the mirror polished cross-sections of the treated AISI 304 austenitic stainless steel monolith at 1173 K for 60 min.

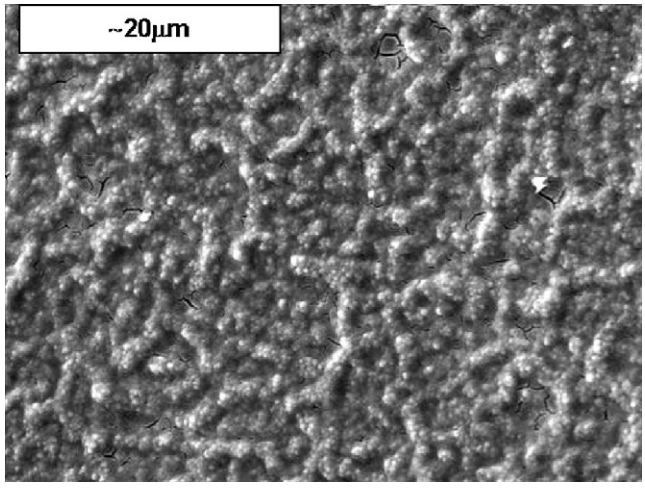

Fig. 4. SEM top view of the austenitic stainless steel surface coated by ceria.

rated and the lower preparation time needed. Besides this, with this method, one can prepare catalytic dispositives with gold incorporated by using exactly the same experimental preparation parameters than those used for the impregnation of supports without gold, allowing to profit of the previous optimization study of such parameters. Gold has demonstrated to be very active for CO oxidation reaction [15–22]. Recently the metal oxide supports such as Al_2O_3 [19], MnO_x [20], Fe_2O_3 [21], $MgO\text{-}Al_2O_3$ [22], CeO_2 [15–17] were found to promote the activity of Au on selective CO oxidation and the catalytic combustion of volatile organic compounds, but among the different metal oxides used as the support of Au for CO oxidation, cerium oxide or ceria (CeO_2) is one of the interesting metal oxides, which may exist in several compositions due to the capacity of Ce to switch between the two oxidation states of Ce^{3+} and Ce^{4+}. In this sense, due to a facile redox reaction cycle, ceria exhibits oxygen storage capacity and improves the CO and hydrocarbon oxidation [15,16]. Also, a number of functions have been ascribed to ceria, including maintaining the dispersion of the catalytic metals [23] and stabilizing the surface area of the support [24]. For alumina, the activity is mainly related with the average size of the gold particles, in such a way that the lower the metal size the higher the catalytic activity [15,18].

3.2.1. Supports coatings

SEM images (Figs. 4 and 5) show the homogeneity of the ceria and alumina layers on stainless steel monolith in where the crack and spalling phenomena are avoided. Ce and Al presence was confirmed by EDX analysis. As can be seen in the figures, the morphology of the coatings is determined by the morphology of the generated oxide layer in which sub-micrometrics crystals are observed.

Two different approaches can be used to evaluate the coating thickness. The first one is the direct measurement using the cross-section SEM views. The significance of this value depends on the number of views used and the certitude that the coating is preserved during the manipulation needed to prepare the sample. This is really difficult when cutting the metal monolith is necessary and some powder is released during the operation corroborating a partial spalling of the coating. Nevertheless, some images where obtained (Figs. 6 and 7) showing thickness from 0.7 to 0.9 μm.

The second approach is to calculate an average thickness based on the amount of coating, the total surface of the metal sheet (240 cm^2 taking into account both sides of the two sheets used to construct a monolith) and the density of the coating. This density data is the critical point because it depends on the bulk density of the oxide, the internal pore volume and the eventual void fraction between particles. In our case, taking into account that the starting material is a diluted colloid and a slow drying procedure is used, we can accept that only the mesoporosity measured by nitrogen adsorption must be considered. Therefore, using calculated coating densities of 1.6 and 6.25 g/cm^3 for alumina and ceria, respectively, average thickness obtained where 2.59 μm for alumina and 0.7 μm for ceria.

Excellent agreement is obtained in the case of ceria and important difference in the case of alumina that could be related with the lower compact character of the alumina due to the higher porosity.

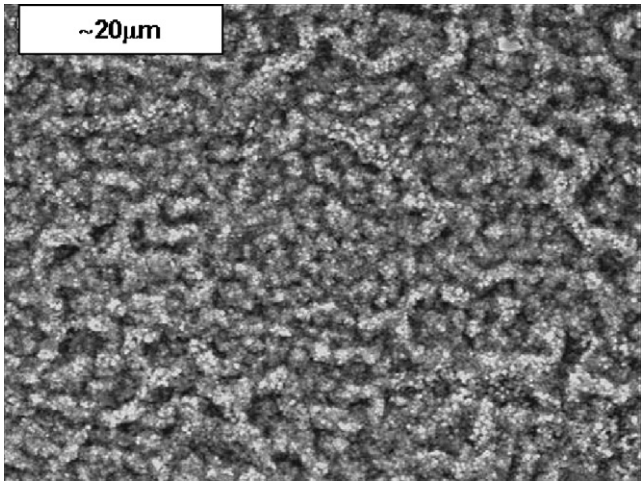

Fig. 5. SEM top view of the austenitic stainless steel surface coated by alumina.

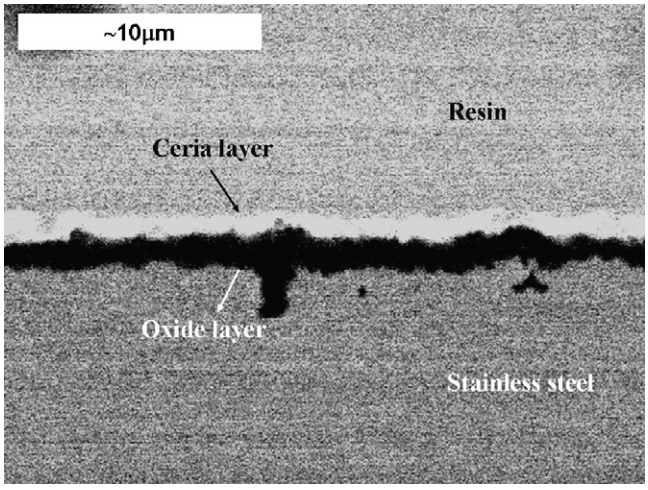

Fig. 6. SEM micrograph of the mirror polished cross-sections of the austenitic stainless steel surface coated by ceria.

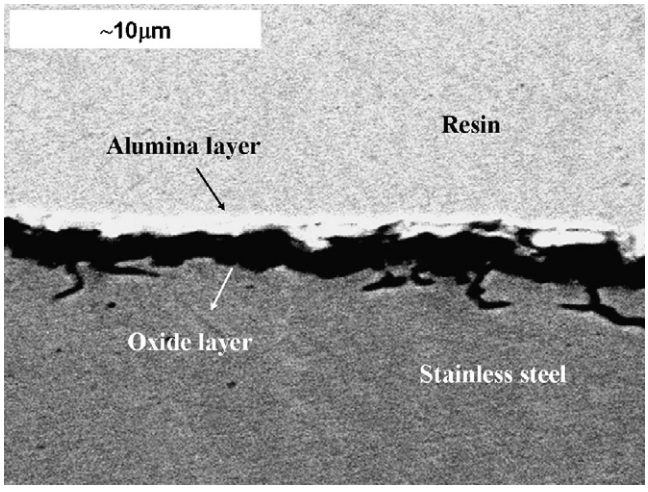

Fig. 7. SEM micrograph of the mirror polished cross-sections of the austenitic stainless steel surface coated by alumina.

XRD results (Fig. 8) confirm that crystalline cerianite has been deposited and also that bohemite → γ-Al_2O_3 transformation occurs after calcination. Table 2 summarizes the textural properties of the coating monoliths with ceria and alumina obtained from N_2 adsorption–desorption isotherms (Fig. 9). The isotherms correspond to typical mesoporous materials with complex pore size structures having average pore radius of 92 and

Table 2
Textural properties of coating monoliths with CeO_2 and Al_2O_3

	Al_2O_3/monolith	CeO_2/monolith
Coating (mg)	91.6	97.1
Adherence test (percentage of the loss of weight of the catalytic layer)	0.9	1.0
S_{BET} (m^2 monolith^{-1})	14	4
S_{BET} (m^2 g catal^{-1})	151	48
Pore volume (cm^3 monolith^{-1})	0.032	0.006
Pore volume (cm^3 g catal^{-1})	0.35	0.063
Pore diameter (Å)	92	53

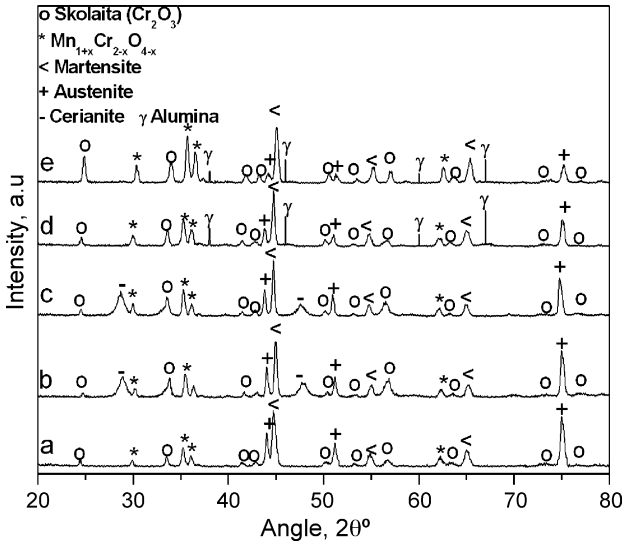

Fig. 8. XRD patterns of AISI 304 austenitic stainless steel monolith: treated at 1173 K for 60 min (a), CeO_2/monolith (b), 0.1% Au-CeO_2/monolith (c), Al_2O_3/monolith (d) and 0.1% Au-Al_2O_3/monolith (e).

53 Å for alumina and ceria, respectively. BET surface areas of the treated monolith without coating are lower than 1 m^2/monolith, but they are increased over 14 and 4 m^2/monolith for alumina and ceria on stainless steel monolith, respectively. Recalculating the surface areas and pore volume only considering the weight of ceria or alumina and not the total weight of the monolith, the obtained values are 151 m^2/g of Al_2O_3 and 0.35 cm^3/g of Al_2O_3 and 48 m^2/g of CeO_2 and 0.063 cm^3/g of CeO_2 for the coating monoliths. Not only BET surface area but pore diameter and pore volume are bigger in monoliths coated with alumina than in those coated with ceria. These observations could be related with the textural properties of the CeO_2 and Al_2O_3 powders obtained after calcinations at 773 K of the corresponding commercial colloids used in the monoliths impregnation [25]. The differences in surface area between alumina and ceria on stainless steel monolith does not affect the excellent adherence

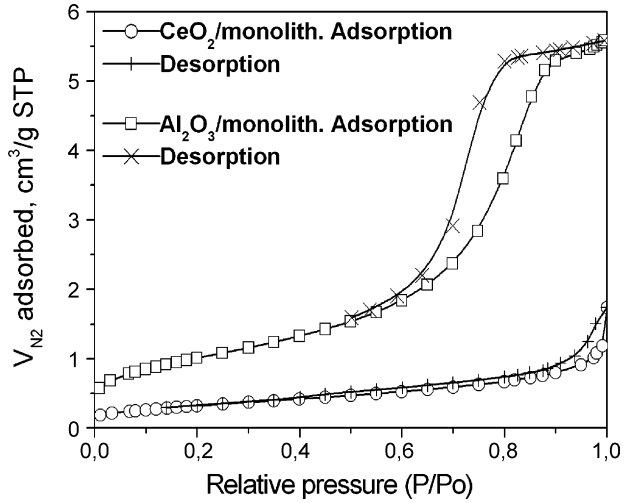

Fig. 9. N_2 adsorption–desorption isotherms obtained for the coating monolith with colloidal ceria and alumina.

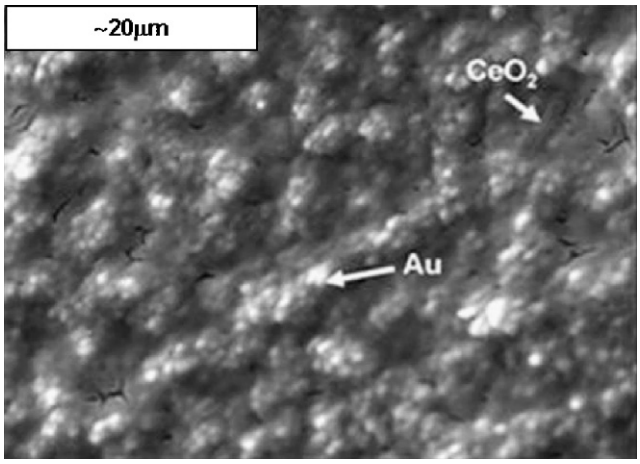

Fig. 10. SEM top view of the austenitic stainless steel surface coated by 0.1% Au-CeO_2.

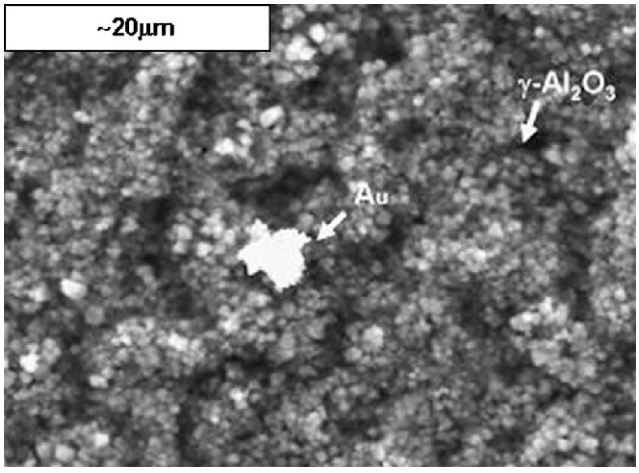

Fig. 11. SEM top view of the austenitic stainless steel surface coated by 0.1% Au-Al_2O_3.

of the active layer to the pre-treated metallic surface being the weight losses ∼1 wt.% after ultrasonic test.

3.2.2. Gold-supported coatings

SEM analysis of the gold-supported monolithic catalysts shows no differences with those devices prepared without gold but the presence of gold clusters (Figs. 10 and 11). The average size of the gold clusters observed on the alumina coating is higher than those detected on ceria one. This observation agrees with the reported preferential deposition of gold over ceria in CeO_2/Al_2O_3 systems, resulting in the deposition of smaller gold particles on the ceria phase [15,25]. The presence of gold does not alter significantly the adherence of the washcoated active phase (∼1.2 wt.%). The thickness of the catalytic layer is similar to that observed for the support coating (0.7–0.9 μm) and EDX analysis evidences the homogeneous presence of gold in the entire layer. The XRD diagrams of the monoliths (Fig. 8, traces c and e) indicate the absence of additional phases apart from gold. Gold could not be detected by XRD in any case, in good agreement with its low percentage and/or crystalline domain size. Once gold is introduced the textural properties of the monolith with ceria are maintained, but with alumina some small changes are observed due to size of gold clusters (Table 3).

3.3. Catalytic activity measures

Figs. 12 and 13 present the activity for the oxidation of CO of the prepared monoliths and catalyst powders in presence and absence of water showed as light off curves. CO conversion for the uncoated monolith is fairly low starting at 673 K for reaching less than 5% conversion at 773 K. Even low the activity has to be associated to the presence of transition metal oxides on the metallic surface [10,25] as results of the thermal treatment for improving adherence.

As expected coating the monolith with alumina (Fig. 12), slightly improves the catalytic performances of the monolithic device but CO conversion only starts over 600 K and never is higher than 40% at 773 K. On the contrary CeO_2-coated monoliths largely improves the catalytic behavior of the AISI 304 monolithic device (Fig. 13), with a T_{50} value (for practical purposes a measure of the activity) of 573 K. Obviously, this behavior is related to the redox properties of CeO_2, which has been proved to increase the catalytic activity of metal-supported catalyst in the CO and VOCs oxidation reactions [15]. Also, CeO_2 can promote the catalytic activity for transition metals (Fe, Cr, Mn) that remain over the surface [10,25].

Gold clearly enhances the catalyst activity in the oxidation of CO. For 0.1% Au-alumina coated monolith (Fig. 12), the conversion reaches 80% at 773 K being the effect of water negative as previously reported [16]. The low increment observed in activity is related with the low gold content deposited and the presence of gold clusters of high size, as observed by SEM. When ceria is use as support, the catalytic activity is highly enhanced (Fig. 13),

Table 3
Textural properties of coating monoliths with Au-CeO_2 and Au-Al_2O_3

	0.1% Au-Al_2O_3/monolith	0.1% Au-CeO_2/monolith	1% Au-CeO_2/monolith
Coating (mg)	93.4	95.6	107.4
Adherence test (percentage of the loss of weight of the catalytic layer)	1.1	1.2	1.2
S_{BET} (m^2 monolith^{-1})	11	4	5
S_{BET} (m^2 g catal^{-1})	121	46	52
Pore volume (cm^3 monolith^{-1})	0.026	0.006	0.007
Pore volume (cm^3 g catal^{-1})	0.28	0.062	0.065
Pore diameter (Å)	93	53	49

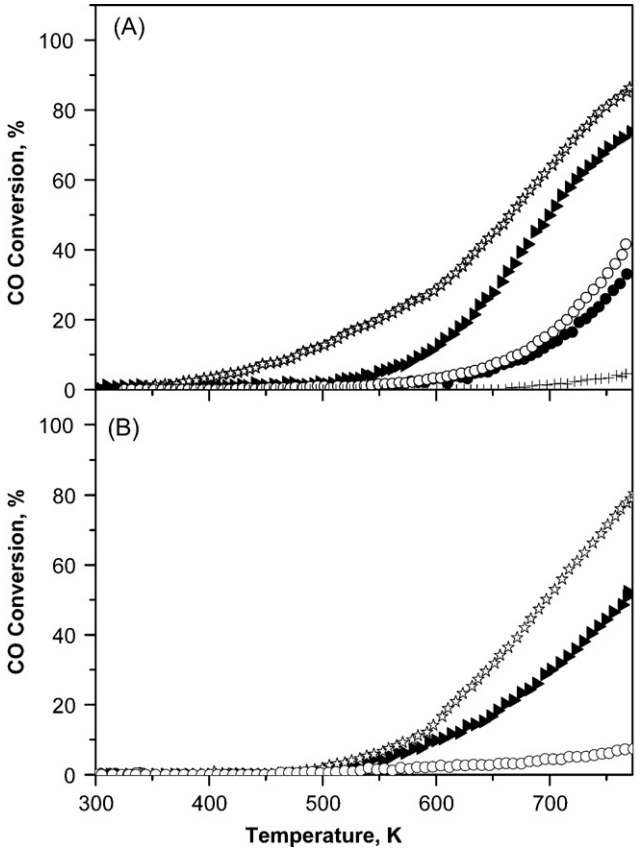

Fig. 12. Water effect on conversion of CO using (A) austenitic stainless steel monoliths with different coatings and (B) powders catalysts. Symbols: 0.1% Au-Al_2O_3 with water (▲) and without water (*); Al_2O_3 with water (●) and without water (◯). Treated monolith without coating (+).

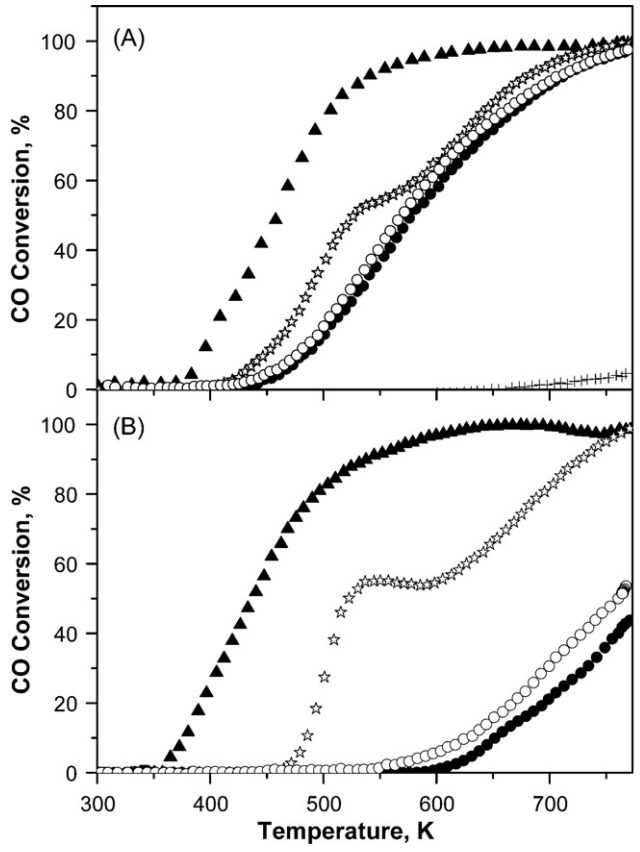

Fig. 13. Water effect on conversion of CO using (A) austenitic stainless steel monoliths with different coatings and (B) powders catalysts. Symbols: 0.1% Au-CeO_2 with water (▲) and without water (*); CeO_2 with water (●) and without water (◯). Treated monolith without coating (+).

either in the presence or absence of water in the reaction stream (T_{50} of 443 and 523 K, respectively).

In the light off curve obtained for 0.1% Au-CeO_2 coated monoliths in absence of water, a shoulder is clearly observed at around 530 K. The presence of shoulders in the CO light off curves has been recently reported in the literature, being its explanation under discussion at the moment [26,27]. Effects of water concentration, cooling atmosphere, changes in the oxidation state of gold, or in the nano-environment of the gold nanoclusters, among others, have been claimed as responsible for the change in the shapes of the light off curves and for the appearance of such shoulders.

Water exerts a clear influence in the redox reactions implied in the catalytic oxidation of CO [16] favoring the mobility of the oxygen species and stabilizing the oxidation state of gold. In this sense, metallic gold are generally considered the active species for the oxidation reaction [28], although oxidized species have also been proposed to contribute to this reaction [17–25,29]. The results indicate that the best results are obtained with ceria and gold thanks to the combination of both effects, the enhanced oxygen storage capacity of the catalysts due to the ceria ability to undergo deep and rapid reduction/oxidation cycles, and the enhanced oxidation performances of the monoliths due to the existence of gold atoms. A similar conclusion has been reported for powdered Au/CeO_2/Al_2O_3 catalysts in the catalytic combustion of volatile organic compounds [15]. On the other hand, SEM micrograph suggests a better dispersion of the gold phase, which also contributes to improve the catalytic performances of the monolith with ceria. Finally, the increase in gold loading clearly improves the catalytic activity (Fig. 14), shifting the T_{50} to values as low as 400 K for 1% Au-ceria coated monolith in the presence of water.

The catalytic activities of both support powder catalysts is always lower than those obtained for the support deposited on the monolithic substrates. This observation must be related with the probably presence of transition metal atoms coming from the oxide scale of the stainless steel treated surface, which has been described as active centers for CO oxidation [25]. A similar situation occurs for gold supported alumina catalysts, where monoliths are more active than powders. This fact confirms the low activity of the gold centers in such catalysts, in good agreement with the high size of the gold clusters observed by SEM.

In the case of gold supported ceria catalysts, little or none differences in activities are detected between monoliths and powders putting in evidence the higher influence of the gold centers. From here, in these solids, the CO oxidation catalytic activity is mainly due to the presence of gold sites.

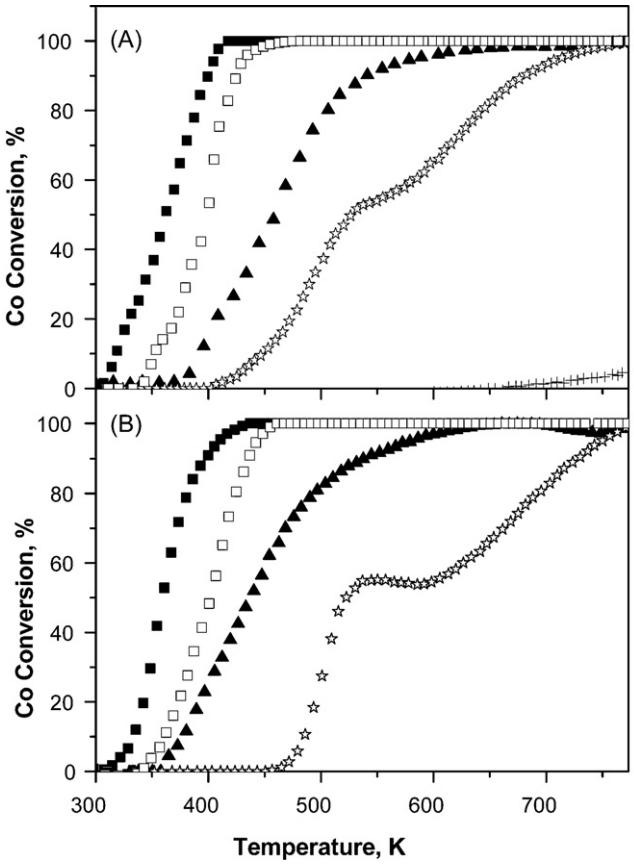

Fig. 14. Gold concentration effect on conversion of CO using (A) austenitic stainless steel monoliths with different coatings and (B) powders catalysts. Symbols: 1% Au-CeO_2 with water (■) and without water (□); 0.1% Au-CeO_2 with water (▲) and without water (*).

4. Conclusion

We have shown that it is possible to use AISI 304 stainless steel sheets as substrate to prepare parallel channels metallic monoliths for catalytic devices with adequate textural and morphological characteristics. The preparation strategy needs a proper metal surface modification by thermal treatment but once this is attained it is possible to deposit a large amount of catalyst. In this work the monolithic devices were coated with colloidal ceria, alumina, Au-ceria and Au-alumina obtaining homogeneous and adherent coatings. The obtained catalytic devices were active to the CO oxidation reaction. The best catalytic results are obtained for 1% Au-ceria where the oxidation capability of gold atoms is combined with the redox properties of the ceria phase.

Acknowledgements

Financial support by Spanish Ministerio de Ciencia y Tecnología-MCYT (MAT2003-06540-CO2), CYTED Programme (PI0269), Programme AlBan-European Union Programme of High Level Scholarships for Latin America (L.M. Martínez T Ph.D. UE E04D046878CO Scholarship) and UJAT-PROMEP-México (D.M. Frías Ph.D. Scholarship) are gratefully acknowledged.

References

[1] R.M. Heck, S. Gulati, R.J. Farrauto, Chem. Eng. J. 82 (2001) 149.
[2] P. Ávila, M. Montes, E.E. Miró, Chem. Eng. J. 109 (2005) 11.
[3] G. Groppi, G. Airoldi, C. Cristiani, E. Tronconi, Catal. Today 60 (2000) 57.
[4] S. Irandoust, B. Andersson, Catal. Rev. Sci. Eng. 30 (3) (1998) 341.
[5] A. Cyulski, J.A. Moulijn, Catal. Rev. Sci. Eng. 36 (2) (1994) 179.
[6] A. Paúl, Ph.D. Thesis, Instituto de Ciencia de los Materiales, Universidad de Sevilla, 1997.
[7] N. Burgos, M. Paulís, M. Montes, J. Mater. Chem. 13 (2003) 1458.
[8] M.J. Capitan, S. Lefebvre, A. Traverse, A. Paúl, J.A. Odriozola, J. Mater. Chem. 8 (10) (1998) 2293.
[9] M.J. Capitan, A. Paúl, J.L. Pastol, J.A. Odriozola, Oxid. Metal. 52 (516) (1999) 447.
[10] X. Han, R. Zhou, G. Lai, X. Zheng, Catal. Today 93–95 (2004) 433.
[11] L.M. Martinez, T.M.A. Centeno, A. Paúl, M. Montes, J.A. Odriozola, Stainless Steel'05 Market and Science, CICIC, España, 2005, p. 303.
[12] A. Paúl, J.A. Odriozola, M.A. San Miguel, J.F. Sanz, L.J. Alvarez, Acta Mater. 48 (2000) 2951.
[13] A. Paul, S. El Mrabet, F.J. Ager, J.A. Odriozola, M.A. Respaldiza, M.F. da Silva, J.C. Soares, Oxid. Metal. 57 (2002) 33.
[14] A. Paúl, J.A. Odriozola, Mater. Sci. Eng. A Struct. Mater. Prop. Micros. Process 300 (2001) 22.
[15] M.A. Centeno, M. Paulis, M. Montes, J.A. Odriozola, Appl. Catal. A 234 (2002) 65.
[16] M.A. Centeno, C. Portales, I. Carrizosa, J.A. Odriozola, Catal. Lett. 3–4 (2005) 289.
[17] M.A. Centeno, K. Hadjiivanov, Tz. Venkov, Hr. Klimev, J.A. Odriozola, J. Mol. Catal. A 252 (2006) 142.
[18] Tz. Venkov, Hr. Klimev, M.A. Centeno, J.A. Odriozola, K. Hadjiivanov, Catal. Commun. 7 (2006) 308.
[19] G.K. Bethke, H.H. Kung, Appl. Catal. A 194 (2000) 43.
[20] R.M.S. Torres, S.A. Udea, K. Tanaka, M. Haruta, J. Catal. 168 (1) (1997) 125.
[21] L. Guczi, D. Horvath, D. Paszti, G. Peto, Catal. Today 72 (1–2) (2002) 101.
[22] R.J.H. Grisel, C.J. Weststrate, A. Goossens, M.W.J. Crajé, A.M. van der Kraan, B.E. Nieuwenhuys, Catal. Today 72 ((1–2)) (2002) 123.
[23] A.F. Diwell, R.R. Rajaram, H.A. Truex, Stud. Surf. Sci. Catal. 71 (1991) 139.
[24] O. Ozawa, M. Kimura, J. Mater. Sci. Lett. 9 (3) (1990) 291.
[25] M.I. Domínguez, M. Sánchez, M.A. Centeno, M. Montes, J.A. Odriozola, Appl. Catal. A 302 (2006) 96.
[26] J.G. Carriazo, L.M. Martinez, T.J.A. Odriozola, S. Moreno, R. Molina, M.A. Centeno, Appl. Catal. B 72 (2007) 157.
[27] E.G. Szabó, A. Tompos, M. Hegedus, A. Szegedi, J.L. Margitfalvi, Appl. Catal. A 320 (2007) 114.
[28] M. Haruta, M. Date, Appl. Catal. A 22 (2001) 427.
[29] Q. Fu, S. Kudriavtseva, H. Satsburg, M. Flytzani-Stephanopoulus, Chem. Eng. J. 93 (2003) 41.